GEOLOGICA CARPATHICA, APRIL 2017, 68, 2, 165–174 doi: 10.1515/geoca-2017-0013

Mapping of tecto-lineaments and their influence on sedimentological processes in a GIS environment: a case study of the Iberian trough, Spain

ANTONIO HERRERO-HERNÁNDEZ[1], FRANCISCO JAVIER LÓPEZ-MORO[2], MARÍA ELENA VALLE-FEIJÓO[3], FERNANDO GÓMEZ-FERNÁNDEZ[1,3] and JOSÉ RAMÓN RODRÍGUEZ-PÉREZ[3]

[1]Research Group of Geological Engineering and Materials (INGEOMAT), Department of Mining Technology, Topography and Structures, Faculty of Mining Engineering, University of Leon, Campus of Vegazana, s/n, 24071 León, Spain; aherh@unileon.es
[2]Department of Geology, Faculty of Science, University of Salamanca, C/ Plaza de Los Caídos s/n, 37008 Salamanca, Spain; fjlopez@usal.es
[3]Department of Mining Technology, Topography and Structures, Faculty of Mining Engineering, University of Leon, Campus of Vegazana, s/n, 24071 León, Spain; miryam.valle@unileon.es, f.gomez@unileon.es, jr.rodriguez@unileon.es

(Manuscript received January 7, 2016; accepted in revised form November 30, 2016)

Abstract: The subsurface sedimentary succession of the Iberian Trough, Spain was examined using geophysical techniques (analogue seismic profiles) and inverse distance weighted (IDW) interpolation algorithm implemented in a gvGIS open source software. The results showed that the Late Cretaceous succession is divided into two depositional sequences: DS-1 (Late Albian–Middle Turonian) and DS-2 (Late Turonian–Campanian). From the analogical seismic sections, digital data and quantitative isopach maps for DS-1 and DS-2 were obtained. The new isopach maps obtained for the DS-1 sequence showed that the deeper sectors of the basin were located to the northeast and the proximal ones to the southwest. The palaeoshoreline was inferred to be situated in the N 150 direction. Across and parallel to this direction several blocks were delimited by faults, with a direction between 30 N and N 65. The thickness of the sediments in these blocks varied in direction NW–SE, with subsidence and depocentres in hangingwall and uplift in the footwall. These variations may have been related to active synsedimentary faults (e.g., Boñar and Yugueros Faults). In the DS-2 sequence, a lineament separated the smaller thicknesses to the southwest from the larger thicknesses (up to 1400 m) to the northeast. This lineament had an N170 orientation and it indicated the position of the palaeoshoreline. In the isopach map for DS-2 there were two groups of lineaments. The first showed a block structure that was limited by N100–120, they were foundering toward the S and had large thicknesses (depocentres), and rose towards the N, where there were smaller thicknesses. The second group of lineaments had a N 50–65 direction and, in this case, they had a similar interpretation as the one in DS-1. The maps obtained are of great help for geologists and permit better understanding of the geological setting and stratigraphic succession of the Late Cretaceous of the Iberian Trough.

Keywords: Iberian Trough, Late Cretaceous, seismic, Isopach maps, GIS, IDW.

Introduction

The understanding of the depositional context and reconstruction of sedimentary basins has become a major topic in earth sciences and is now a necessary step for modelling the data in subsoil. In the study area, the surface data were generally scattered, and it was necessary to collect the data from the subsoil. Geophysical methods, mainly seismic and well-logging are routinely used in studies of subsurface analysis (see Galloway 1989; Herrero-Hernández et al. 2004; Catuneanu et al. 2009, 2011). Less frequently, a combination of these methods of subsoil analysis along with GIS (Geographical Information System) techniques and geostatistical techniques are employed (see Cheng-Shin et al. 2013; Jurecka et al. 2016). However, they are usually applied in the cartographic mapping of the earth's surface and they provide this data in a relatively quick and non-expensive manner.

In the literature for geosciences there is an abundance of works that apply digital elevation models (DEM) and remote sensing images in order to obtain data about the geological and morphotectonic structure (see Chorowicz et al. 1998, 1999; Collet et al. 2000; Elmahdy & Mohamed 2016a). DEMs are used (i) to calculate the dip and strike of the strata (Chorowicz et al. 1991), (ii) to define the geometry of the fault plane (Koike et al. 1998; Jordan et al. 2005), (iii) to define morphotectonic parameters, such as the slope of the terrain, curvature of the profile, etc., (Burbank & Anderson 2001; Keller & Pinter 2002; Nappi et al. 2009; Elmahdy et al. 2012). The relationship between the morphology of the terrain and the tectonic deformation with geophysical data (seismic) has been analysed in some works by using GIS techniques (e.g., Jordan et al. 2005; Nappi et al. 2009).

The classical approach to the integration of digital methods with geomorphology and tectonics includes the identification of linear faults, definition of patterns of the drainage network, identification of linear valley crests and linear slope breaks, among other morphological expressions. Interpolation methods are widely used for groundwater contour maps, but can also be used to attribute 2D information, and to create representations such as maps that show the concentration of contaminants.

However, the application of using geostatistics and GIS technologies in order to study the geology of the subsoil is relatively novel, and its development is still incipient in many fields. The application of GIS technologies for the analysis of the potential for hydrocarbons is usually done with a large dataset, and map layers such as aerial photos or satellite imagery (raster data) and hydrology, elevation contours, and topographic landmarks (vector data) (e.g., Jordan et al. 2005; Nappi et al. 2009).

In this paper, the powerful tools of a GIS for the analysis of the spatial and temporal (3D-4D) variation, which are frequently used in the exploitation of hydrocarbons, were used to keep track of the spatial and temporal variations of the isopach maps of the lithoseismic units. This was a difficult task for the study area that was used in this research. First, the Mesozoic sediments, which were the object of this work appeared on the surface in a narrow band below 5 km and were around 60–80 km long, and had an East-West orientation and were located on the north side of the study area. Second, the geological maps in the region (see Gómez-Fernández et al. 2003) allowed for the identification of tectono-structural patterns that had an apparent continuity in the basement. Third, the initial data were printed in seismic sections on paper, so digital data was not obtained. Therefore the data could not be used for other basic methods such as the analysis of the subsoil to model reservoirs, e.g., inverse geostatistical methods (e.g., Grijalba-Cuenca et al. 2000), which uses the variability in any petrophysical parameter such as porosity, permeability, etc.

The main objective of this study is to map tecto-lineaments cross-cutting the late Cretaceous Iberian Trough and investigate their influence on the sedimentological process.

Study area

The area under investigation is located in the province of Leon, Spain. It stretches between latitude 4760000(N) and 4680000(S), and longitude 260.000(W) and 390.000(E) (coordinates ETRS89/UTMzone30N). In the Iberian Peninsula, from the Jurassic to Late Cretaceous period, an extensional sedimentary basin (Iberian Trough) was created. The study area is located in the western margin of a Mesozoic extensional sedimentary basin (Iberian Trough), namely in the so-called Leonese Area. The crystalline basement consists of Palaeozoic units and belongs to the Variscan Domains of the Cantabrian Mountains (Cantabrian Zone and West-Asturian-Leonese Zone) (Fig. 1).

According to the litho-stratigraphic successions (Fig. 2), the sediment thickness is between 150 and 650 m and transgression and regression stages are inferred by changes of fluvial to tidal flat and shallow marine deposits.

Several previous studies (e.g., Gómez de Llarena 1934; Ciry 1939; Evers 1967; van Ameron 1965; Jonker 1972; Gómez-Fernández et al. 2003; Herrero-Hernández et al. 2010, 2013) have been applied to describe the Late Cretaceous successions in the study area. The general stratigraphic organization is composed of two lithostratigraphic units: the Voznuevo Member and the Boñar Formation (Fig. 1). Between these units, a lateral shift of lithology from detrital-carbonate materials (east) to exclusively detrital materials (west) took place.

The Voznuevo Member essentially consists of white, reddish and yellow ferruginous sandstones. Its thickness ranges from 350 m in the west to 150 m in the middle part of the study area. The Voznuevo Member is mainly characterized by deposits derived from different fluvial systems that drained this part of the Iberian Massif.

The Boñar Formation is mainly formed of carbonate rocks (limestones and dolomites) intercalated with shales and marlstones with thickness of approximately 300 m. This succession indicates that the formation was deposited in terrigenous-carbonated mixed platforms with shallow subtidal and intertidal areas on open shelf depositional environments (Gómez Fernández et al. 2003; Herrero-Hernández & Gómez-Fernández 2012; Suárez-González et al. 2016). The palaeogeography of the study area has not been investigated in details due to the limitations of outcrops. Thus, it is important to include subsoil analysis in order to draw an image of the palaeogeography and palaeotectonics of the sedimentary basin.

Limited numbers of studies (e.g., Herrero-Hernandez et al. 2004, 2010, 2013) have been done using subsoil analysis to build a regional stratigraphic succession in terms of four seismic units: Palaeozoic Seismic Unit, Mesozoic Seismic Unit, Palaeogene Seismic Unit and Neogene Seismic Unit. These units correspond to higher-order sequences in the hierarchy of stratigraphic sequences.

Other studies (e.g., Herrero-Hernández & Gómez-Fernández 2012) conducted using seismic analysis coupled with sedimentological data allowed us to assign two low-frequency signals (2nd and 3rd order) to two depositional sequences in the Mesozoic Seismic Unit: DS-1 and DS-2 (Fig. 3). The stratigraphic cyclicity is based on systems tracts and exhibits remarkable eustatic control (Fig. 3).

Data and methods

A GIS system was implemented and was used to process and generate original informational layers, namely digital isopach maps and maps of new sedimentary and structural lineaments that were obtained from the analysis and interpretation of raster images. These lineaments are linear features created by tectonic activity that reflects linear geological structures, frequently long in length, like faults, joints, aligned ridges, etc. It is noteworthy that during the processing the geophysical data were incorporated into the GIS environment.

Two types of complementary techniques were also employed. First, subsurface techniques were used to obtain the database by seismic reflection for the DS-1 and DS-2 depositional sequences. Seventeen 2D seismic reflection (Fig. 1) analogue profiles with a total length of around 800 km were

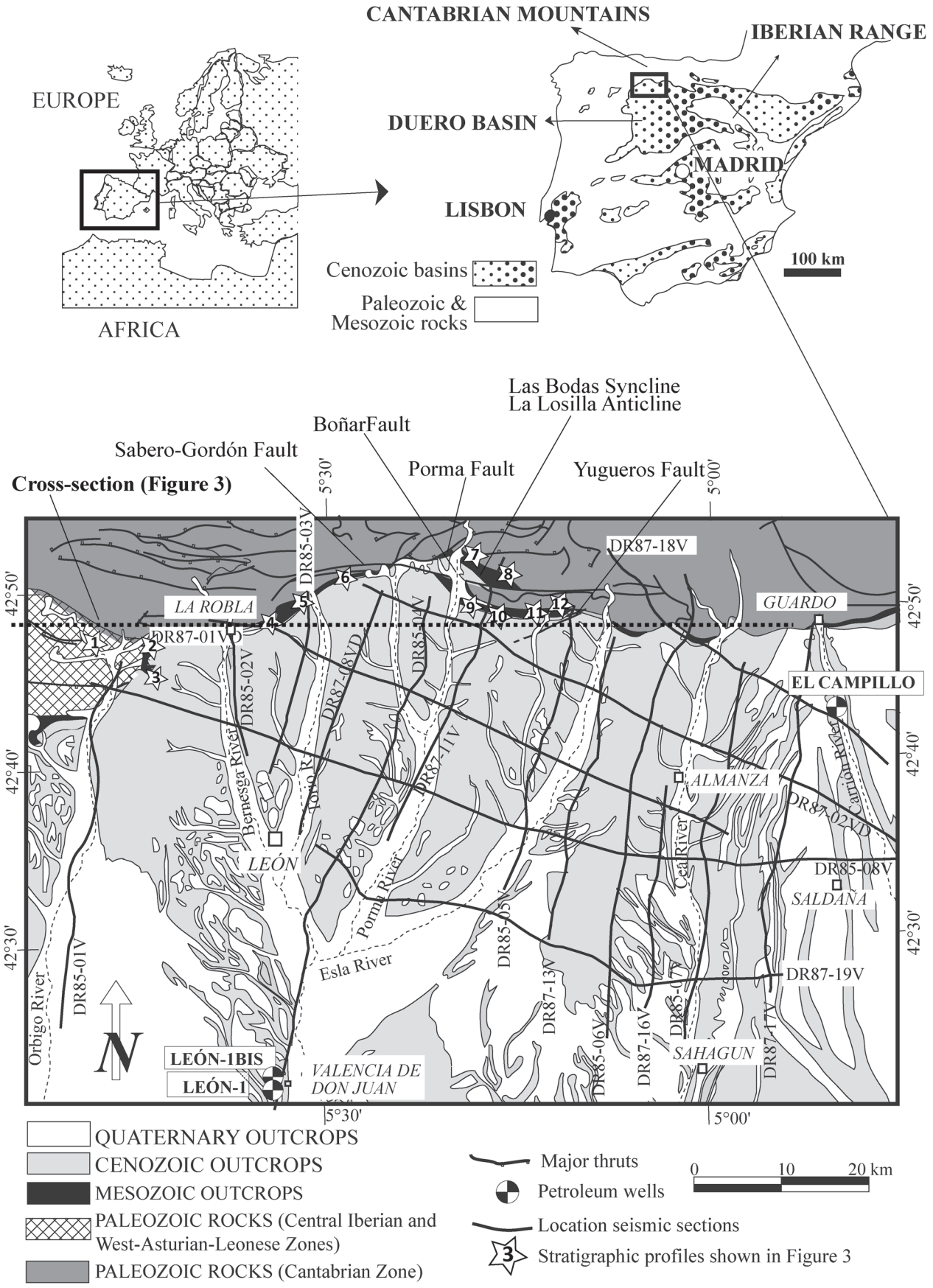

Fig. 1. Regional and geological maps of the study area.

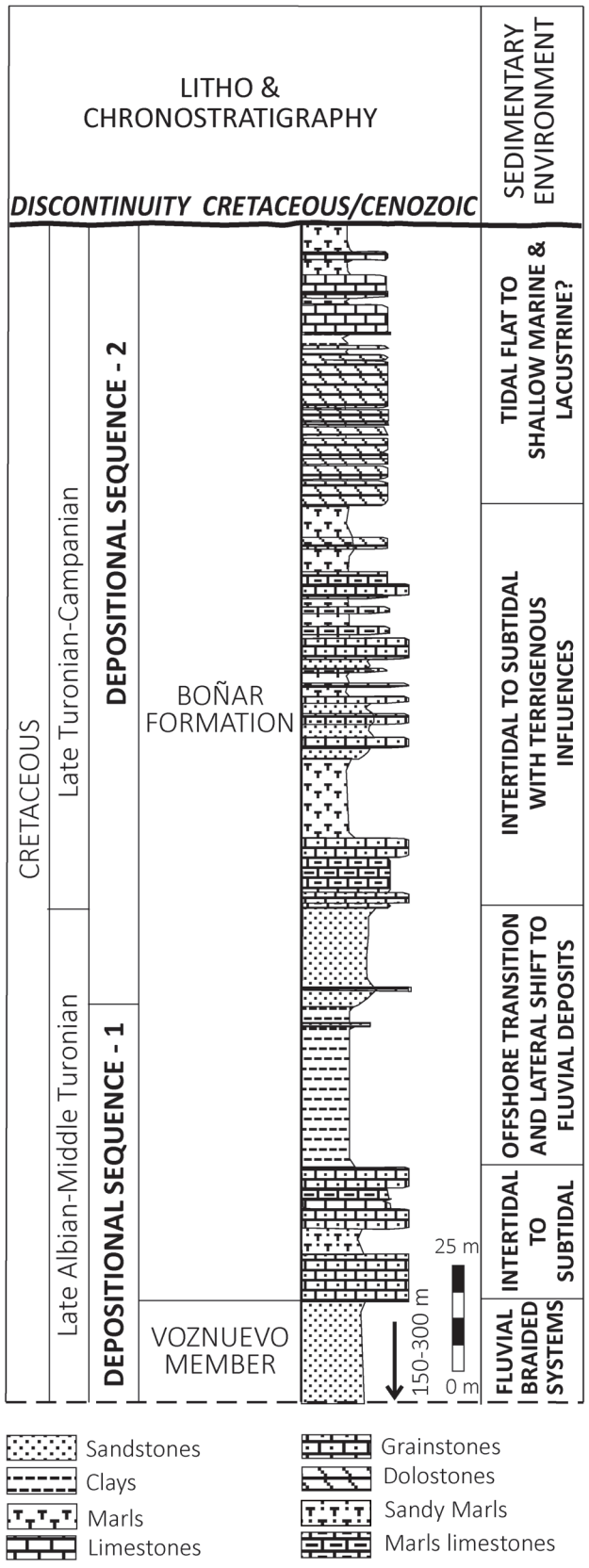

Fig. 2. Stratigraphic profile and depositional environments of the Boñar Formation. Modified after Gómez-Fernández et al. (2003) and Suárez-González et al. (2016).

used. These seismic sections covered an area of about 6000 m^2. The multi-channel seismic data were acquired with vibroseis 3 (WESTERN RICERCHE) and 4 (HISPANOIL). The receiving array consisted of 36 geophones per group, the centre of each group was spaced either 60 or 40 m apart. The duration of the recordings (trace length) was either 15 or 5 s, with a sampling rate of 2 ms. The coverage was 2400 % of the depositional sequences.

Seismic data interpretation starts with the identification of the different horizons in the seismic sections. This method was performed for all the seismic sections, where coordinates were manually taken for each set of points. As a first step, it is important to convert the seismic travel- time data to depth and stack velocity intervals to be taken into account. This coverage allowed contour maps (two way travel time, iso-velocity, isobaths and isopachs) of the depositional sequences to be produced.

Second, a GIS analysis (e.g., gvSIG open source, http://www.gvsig.org/web/), was performed by integrating and overlaying several layers. First, a layer with the location of the shot points and wells was implemented. These points were not spread evenly throughout the region, but they were arranged randomly. A sufficiently extensive network of sampling points were set up in order to be able to interpolate and model the spatial pattern of the isopachs of the depositional sequences, and thus generate information for areas that lacked data. In particular, 271 points were used for each of the depositional sequences.

Isopach maps and faults maps for DS-1 (Late Albian-Middle Turonian) and DS-2 (Late Turonian-Campanian) were obtained. The overall objective was to describe and evaluate the changes in the isopachs and faults during the DS-1 and DS-2 using interpolation techniques. The latter was digitized and superimposed on the former in order to correctly display the geological structure.

Spatial prediction methods that enable data to be predicted for areas in which no data exist are called interpolation methods. There is a wide variety of classic interpolation methods that can be applied to the mapping of continuous surfaces, such as Radial Basis Functions, polygons from Voronoi-Thiessen, inverse distance weighting (IDW), and different types of kriging. Also, new interpolation methods that use lines as basic data have been proposed for geosciences (Gossel et al. 2012).

The reliability of the contour maps is directly dependent upon the total density of control points, as well as the uniformity of their distribution. A goodness of fit, specifically the Kolmogorov-Smirnov (K-S) test, was carried out in every data set to check whether the distribution of isopach values in DS-1 and DS-2 was normal. In the case of an anomalous distribution of isopach values the use of techniques like IDW would be necessary. The simplicity of IDW and the availability of a complete set of extensions integrated into the gvSIG software to obtain the interpolated raster for the IDW were crucial points for using the IDW against the kriging technique.

The data for the 3D-4D analysis were obtained with the gvSIG software, which first generated a georeferenced vector

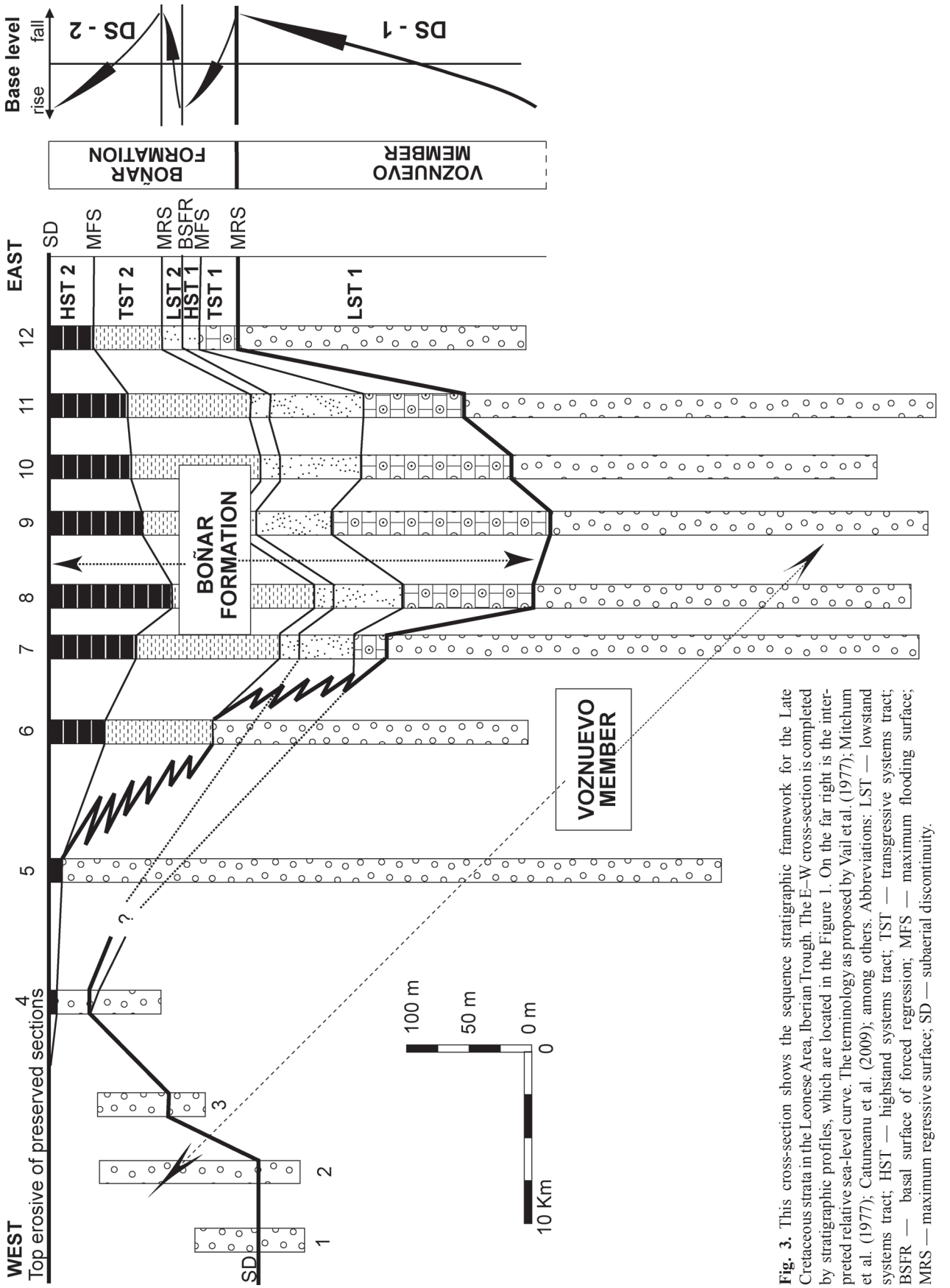

Fig. 3. This cross-section shows the sequence stratigraphic framework for the Late Cretaceous strata in the Leonese Area, Iberian Trough. The E–W cross-section is completed by stratigraphic profiles, which are located in the Figure 1. On the far right is the interpreted relative sea-level curve. The terminology as proposed by Vail et al. (1977); Mitchum et al. (1977); Catuneanu et al. (2009); among others. Abbreviations: LST — lowstand systems tract; HST — highstand systems tract; TST — transgressive systems tract; BSFR — basal surface of forced regression; MFS — maximum flooding surface; MRS — maximum regressive surface; SD — subaerial discontinuity.

layer in shape format that depicted shot points and wells, each with their coordinates and thickness. The reference system EPSG: 25929 (ETRS89/UTMzone29N) was used. The values were subsequently imported into the gvSIG software as a new georeferenced layer, after the interpolation process was conducted.

The IDW method simply means that the arbitrary value of an unsampled point is the weighted average of the known values within the neighbourhood. As is well known, the weights in this method are a function of the radial distance between the observed data points and the estimated point. The weights are inversely related to the distances between the sampled locations and the predicted locations (Lu & Wong 2008).

The spatial modelling was performed with the IDW interpolation method, the formula being:

$$Z(s_0) = \sum_{i=1}^{n} \lambda_i * Z(s_i) \quad (1)$$

where $Z(s_0)$ is the predicted value for the location S_0, n is the number of sampling points close to S_0 and which will be taken into account when the calculation is performed, $_i$ is the weight assigned to each sample point and $Z(s_i)$ is the observed value of the location S_i.

The weights were determined by the equation:

$$\lambda_i = d_{i0}^{-p} / \sum_{i=1}^{n} d_{i0}^{-p} \quad (2)$$

where d_{i0} is the distance between the location which will be interpolated, S_0, and each sample location, S_i, as the distance becomes larger, the weight is reduced by a factor of p. IDW is a method that produced minor differences between observed and projected data for several previous studies (Isaaks & Srivata 1989; Webster & Oliver 2001; Sertel et al. 2007; Krivoruchko 2011). Several trials were conducted and those parameters that produced the smallest errors in the predicted value were used. Because the separation between the shot points of the seismic sections was high the input configurations of the settings, which were loaded into gvSIG, were an exponent 2.0 and an inspection radio of 30 km. A smoother raster was obtained taking into account data to interpolate within this radius.

Once the isopach maps of DS-1 and DS-2 (Figs. 4 and 5) were produced, several structural lineaments could be interpreted. The produced lineaments map and structural analysis were performed. The analysis was carried out by identifying lineament and palaeochannel orientations. This analysis is of great help for geologists to draw an image of the palaeogeographic and sedimentological features as well as the location of the main depocenters of the basin.

Several techniques have been developed to map lineaments using automated algorithms (see Casas et al. 2000; Ekneligoda & Henkel 2010; Elmahdy et al. 2012; Elmahdy & Mohamed 2016b). However, the lineaments were drawn manually, taking into account previous works that were carried out in the same area (Herrero-Hernández et al. 2010, 2013 and Herrero-Hernández & Gómez-Fernández 2012). This process made it possible to incorporate the different lineaments into the digital isopach maps of DS-1 and DS-2. This was done in order to interpret the data from a tectonic and sedimentological point of view, which will be analysed in the following section.

Results and discussion

The quantitative digital isopach map of DS-1 is shown in Fig. 4. The values lower than 140 m thicknesses were located in the west and southwest sectors. The lineament in the N150 direction that curves towards the NW (Fig. 4), represents the enclosure of the 140 m thick isoline and delimits those sectors. This lineament was located in the SW sector of the study area and it exemplifies the position of the palaeoshoreline during the DS-1.

Northeast of the N150 trending lineament, the thickness of the sediments was observed to be changed between 100 m and 950 m. Furthermore, there is a set of corridors and/or palaeo-channels crosscutting and perpendicular to the N150 lineament. These corridors were delimited by faults with directions ranging between N50 and 65 (Fig. 4) that defined the blocks and the formation of the sub-basin where the thickness of the sediments varied in the direction NW–SE. Thickness variations may be due to active synsedimentary faults with N50–65 direction. Some of them were a prolongation of what appeared on the surface, as in the cases of the Yugueros and Boñar Faults (Fig. 4). However, other faults are subsurface in type and have limited outcrops and unclear surface criteria. Both the faults and their prolongation in the basement, as well as some more faults scattered in the subsurface of the region constituted a model for the DS-1, consisting of blocks that were delimited by these faults, falling toward the NW, where they were thicker and rising in the SE part, where they were thinner.

The tectonic process is related to the phase of an extensional basin that produced an array of predominantly normal and dip-slip faults, which generated a hangingwall subsidence and a footwall uplift. The hangingwall subsidence and E and NE palaeocurrents allow us to interpret the occurrence of the large depocentres and faults with an orientation of N50–65. These faults may be linked with the incised valleys and interfluves that were created in these areas. The position of the palaeoshoreline (N150), the mouth of the fluvial systems in the marine basin that was located close to the NE, and the evolution of the sea level during the Late Cretaceous period generated sequence boundaries, system tracts and other scenarios for sedimentation in a continental and coastal/marine setting.

Figure 5 shows the new isopach map that was obtained from the DS-2. A clear line in the N170 direction, which coincides with the position of the 160 m isoline (Fig. 5), separates the thinner area to the southwest from the thicker area (up to 1400 m) to the northeast of this line. This lineament

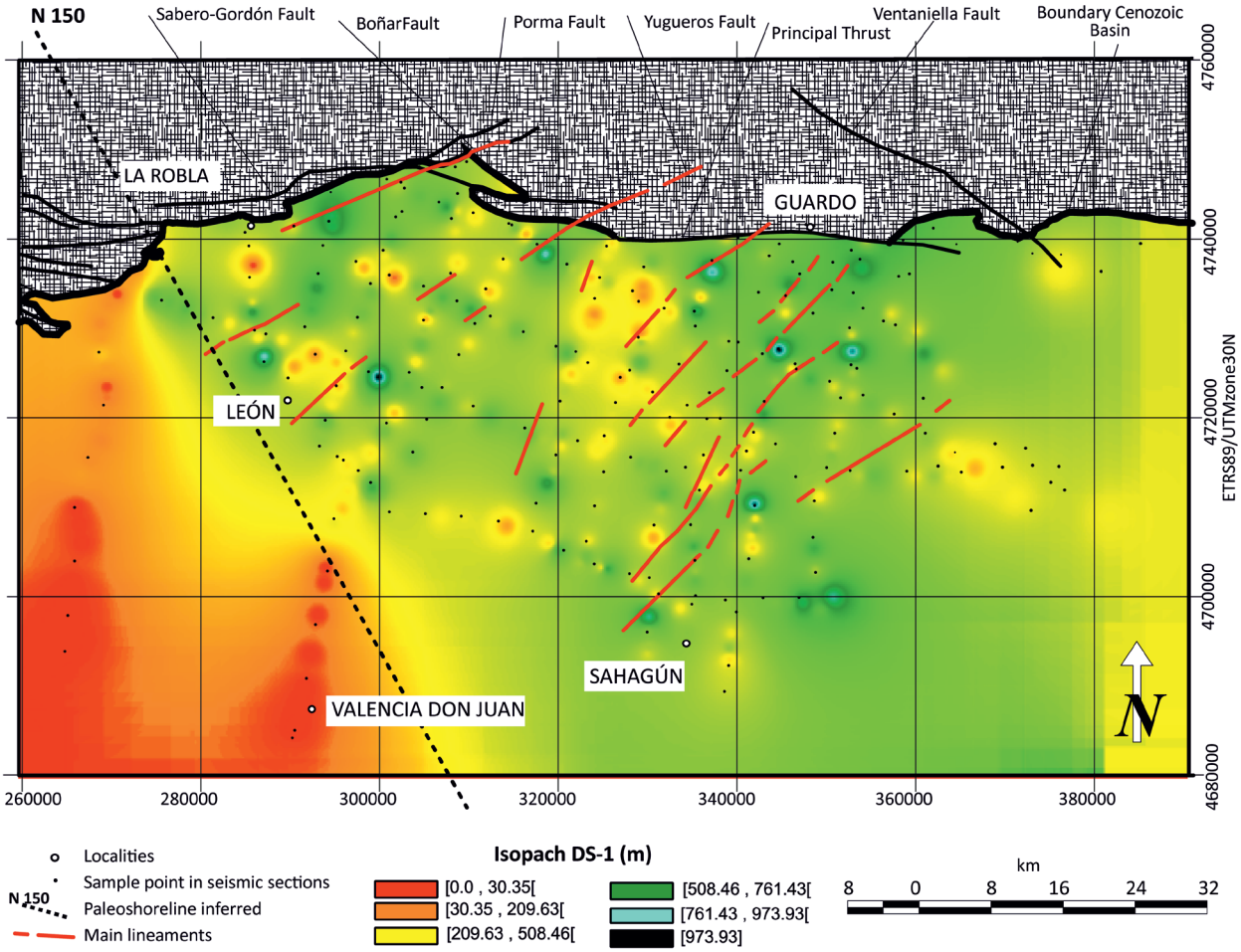

Fig. 4. Isopach map of the DS-1 interpolated from geophysical data using the IDW algorithm (Inverse Distance Weighting interpolation). The N18 to N70 lines (dashed in general) are lineaments that represent a change in the thickness of the sediments. The N150 line represents the position of the palaeoshoreline inferred for the DS-1.

indicates the position of the palaeoshoreline during the DS-2, and it has rotated about 20 degrees in relation to its position during the DS-1. The palaeoshoreline was transgressive and showed a tendency to move landward during DS-2.

On the isopach map of the DS-2, two sets of lineaments can be distinguished (Fig. 5). The first system, with lineaments N100–120, is widespread in the area, and they define sub-basins that are more than 700 m thick in the northern area (Fig. 5) and have a thickness of less than 200 m in the southern area. It is inferred that there is a block structure limited fault N100–120, which sinks towards the S making it thicker, and it rises towards the N where it is thinner.

The second group of lineaments has a N50–65 direction, is less extensive, and is located in the NW area of the basin. Some lineaments appear on the surface and are identified with the Yugueros and Boñar Faults (Fig. 5). The block bounded by the Yugueros and Boñar faults seem to show a thinner area in the SE, and thicker area in the NW that is in coherence with the observation of a significant decrease in the thickness of the sediments in the Yugueros Fault (e.g., Gómez-Fernández et al. 2003). Their interpretation was similar to that given by the DS-1.

It can be drawn that the DS-1 and DS-2 depositional sequences showed periods of lowstand followed by two important transgressions, which were indicated by significant lateral changes of facies and shoreline shifts. The overall shoreline retreat landward was associated with the transgressive units and were more than 10 km to the west.

During the Late Cretaceous epoch an evolution in the tectonic structure of DS-1 and DS-2 occurred. This evolution manifested itself in a gradual disappearance of the NE–SW fault system, that was located in DS-1, and which was circumscribed to the NW area by the prolongation of the Boñar and Yugueros Faults in DS-2. Likewise, in DS-2 inverse faults with a N100–120 direction were formed and reactivated during the Cenozoic period, resulting in thrusts and faults and the formation of a foreland basin, the Duero Basin, in response to the tectonic uplifting of the Cantabrian Mountains. The Cenozoic Duero Basin was filled up with 3500 m of Oligocene and Miocene continental deposits (see Herrero-Hernández 2002; Herrero-Hernández et al. 2004, 2010),

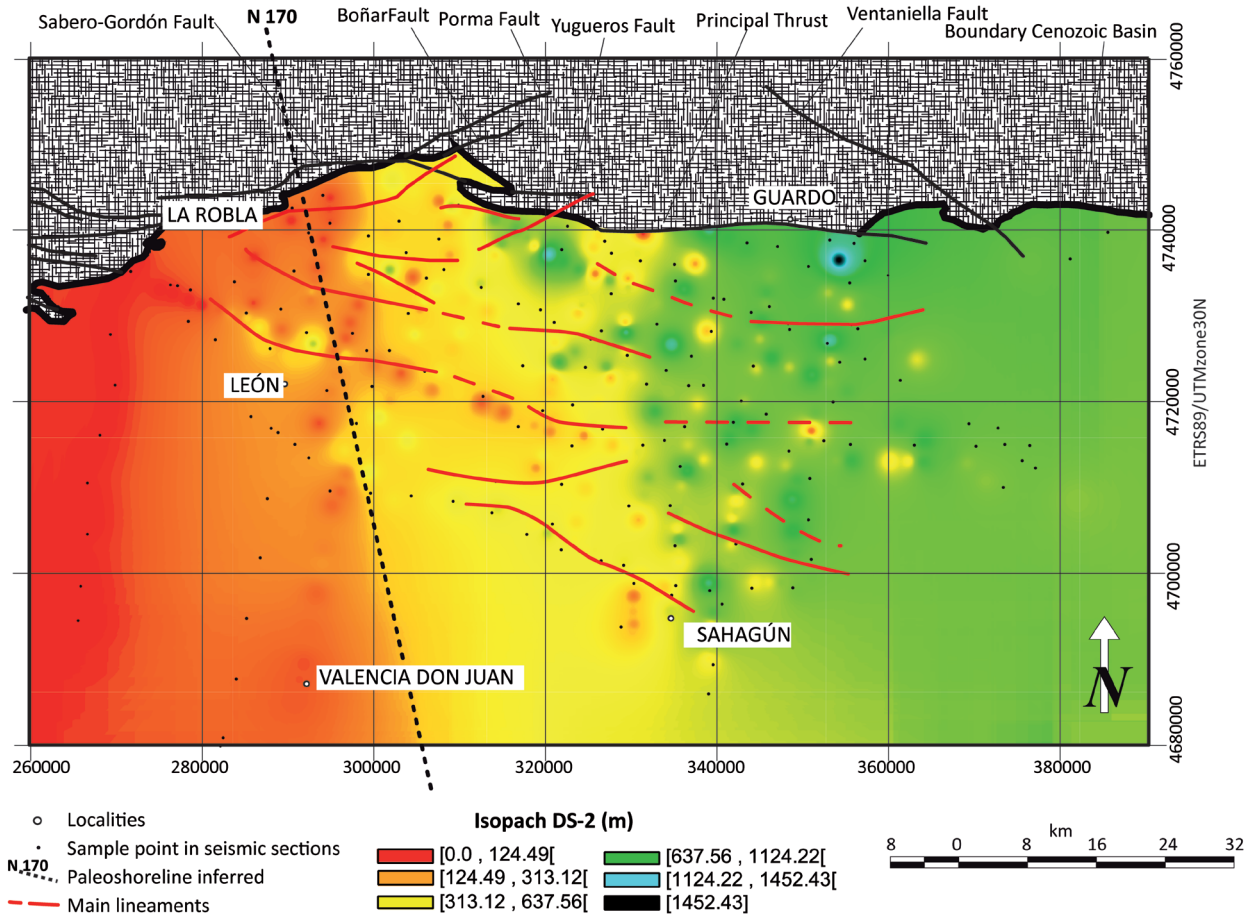

Fig. 5. Isopach map of the DS-2 interpolated from geophysical data and using the IDW algorithm (Inverse Distance Weighting interpolation). The N100 to N120 lines (dashed in general) are lineaments that represent a change in the thickness of the sediments. The N170 line represents the position of the palaeoshoreline inferred for the DS-2.

mostly from the Cantabrian Mountains. These faults indicated (i) the initiation of the phase of the Alpine orogeny with compressive activity in DS-2 and (ii) the cessation of the activity on the faults with the N 50–65 direction, except in the NW area.

The collision of India, Arabia and Africa with Asia and Europe formed the Alpine-Himalayan Belt, in which the westernmost parts are the Pyrenean and Cantabrian Ranges (see Dercourt et al. 1986). Previously, during the Mesozoic post-rifting, Africa shifted its motion northwards, which initiated a convergence with Eurasia. This event was placed towards the end of the Late Cretaceous (chron 33, 80 Ma) (see Dercourt et al. 1986; Vergés & Fernández 2006). In this sense, the compression phase that was found in DS-2 can be equivalent to this event.

Conclusions

The acquisition, processing, and interpretation of seismic data enabled subsurface geological structures to be interpreted. Detailed deep tectonic-structural and sedimentological data and isopach maps obtained for depositional sequences from the seismic acquisition and GIS techniques could be interpreted.

The geological model reconstructions comprised two depositional sequences as well as maps of the tectonic lineaments that were interpreted taking into account the correlation with the surface geology data. Two depositional sequences, the DS-1 sequence (Late Albian–Middle Turonian) and the DS-2 sequence (Late Turonian–Campanian) could be defined in the subsurface architecture.

The results obtained using the IDW interpolation algorithm is much more suitable than the results of the goodness of fit tests that showed the values were not normally distributed. The obtained interpolated maps clearly revealed a set of lineaments with different palaeogeographic and tectonic interpretations. The depocentres were initially related to faults and the associated palaeogeographic thresholds. These appear to be due to thickness variation, horst and graben and fault displacements controlled by the basement.

The most striking tectonic structures in the Late Cretaceous successions were the Las Bodas Syncline and the La Losilla Anticline, with a NW–SE orientation on their axial surfaces, and up to four important faults, namely the Sabero-Gordón Fault, the Porma Fault, the Boñar Fault and the Yugueros

Fault. Some of them were reactivated during the Cenozoic. These tectonic structures were thought to have controlled the sedimentary features and palaeocurrents in the Late Cretaceous period. The results provide better constraints on the geometry of the fluvial palaeochannels of the Late Cretaceous successions and it can be used to better understand the geological evolution in response to sea-level fluctuations.

The interpolated maps using the IDW algorithm in a GIS environment allowed better mapping of palaeoshorelines, with an overall NW–SE direction that changed from N150 (DS-1) to N170 (DS-2), and stratigraphic correlation indicating NW–SE fault displacements.

The palaeoflow directions of the fluvial channel networks and the observation of the corridors with a direction that was orthogonal to the position of the coastline indicated that the fluvial systems were transversal to the previous existing coastlines. The factors that controlled the sedimentation processes were the result of a combination of eustatic changes and tectonic controls that were related to faults with syn-sedimentary activity.

In conclusion, this study integrated geophysical survey and a GIS to map major subsurface lineaments cross-cutting the entire area. Their common trends were found to be in the NW–SE directions, allowing us to interpret the evolution of the depositional sequences and their sedimentological and tectonic characteristics during the Late Cretaceous. These were marked by spatial variation in thickness related to active synsedimentary faults (e.g., Boñar and Yugueros Faults).

Acknowledgements: The support of the members of the INGEOMAT Research Group (University of León) is gratefully acknowledged. We gratefully appreciate careful and detailed reviews by two anonymous reviewers. We thank Ján Madarás for editorial handling.

References

Burbank D.W. & Anderson R.S. 2001: Tectonic Geomorphology. *Blackwell Science*, 1–247.

Casas A.M., Cortes A.L., Maestro A., Soriano M.A., Riaguas A. & Bernal J. 2000: LINDENS: A program for lineament length and density analysis. *Comput. Geosci.* 26, 9–10, 1011–1022.

Dercourt J., Zonenshain L.P., Ricou L.E., Kazmin V.G., Le Pichon X., Knipper A.L., Grandjacquet C., Sbortshikov I.M., Geyssant J. & Lepvrier C. 1986: Geological evolution of the Tethys belt from the Atlantic to the Pamir since the Lias. *Tectonophysics* 123, 241–315.

Ekneligoda T.C. & Henkel H. 2010: Interactive spatial analysis of lineaments. *Comput. Geosci.* 36, 8, 1081–1090.

Catuneanu O., Abreu V., Bhattacharya J.P., Blum M.D., Dalrymple R.W., Eriksson P.G., Fielding G.C.R., Fisher W.L., Galloway W.E. & Gibling M.R. 2009: Towards the standardization of sequence stratigraphy. *Earth-Sci. Rev.* 92, 1–33.

Catuneanu O., Galloway W.E., Kendall C.G.St.C., Miall A.D., Posamentier H.W., Strasser A. & Tucker M.E. 2011: Sequence stratigraphy: methodology and nomenclature. *Newsletters on Stratigraphy* 44, 3, 173–245.

Cheng-Shin J., Shih-Kai C. & Yi-Ming K. 2013: Applying indicator-based geostatistical approaches to determine potential zones of groundwater recharge based on borehole data. *Catena* 101, 178–187.

Chorowicz J., Breard J., Guillande R., Morasse C., Prudon D. & Rudant J. 1991: Dip and strike measured systematically on digitised three-dimensional geological map. *Photogramm Eng. Rem. S.* 57, 431–436.

Chorowicz J., Collet B., Bonavia F.F., Mohr P., Parrot J.F. & Korme T. 1998: The Tana basin Ethiopia: intra-plateau uplift rifting and subsidence. *Tectonophysics* 295, 351–367.

Chorowicz J., Dhont D. & Gundogdu N. 1999: Neotectonics in the eastern North Anatolian fault region (Turkey) advocates crustal extension: mapping from SAR ERS imagery and Digital Elevation Model. *J. Struct. Geol.* 21, 511–532.

Ciry R. 1939: Etude géologique d'une partie des provinces de Burgos Palencia León et Santander *B. Soc. Hist. Nat.* 74, 1–528.

Collet B., Taud H., Parrot J.F., Bonavia F. & Chorowicz J. 2000: A new kinematic approach for the Danakil block using a Digital Elevation Model representation. *Tectonophysics* 316, 343–357.

Elmahdy S.I. & Mohamed M.M. 2016a: Automatic Feature Extraction Module for Change Detection in Al Ain, UAE: Analysis by Means of Multi-temporal Remote Sensing Data. *Journal of the Indian Society of Remote Sensing* 44, 1–10.

Elmahdy S.I. & Mohamed M.M. 2016b: Mapping of tecto-lineaments and investigate their association with earthquakes in Egypt: a hybrid approach using remote sensing data. *Geomatics, Natural Hazards and Risk* 7, 600–619.

Elmahdy S.I., Mansor S., Huat B.B. & Mahmod A.R. 2012: Structural geologic control with the limestone bedrock associated with piling problems using remote sensing and GIS: a modified geomorphological method. *Environ. Earth Sci.* 66, 8, 2185–2195.

Evers H.J. 1967: Geology of the Leonides between the Bernesga and Porma rivers. Cantabrian Mountains NW Spain. *Leidse Geol Mededelingen* 41, 83–151.

Galloway W.E. 1989: Genetic stratigraphic sequences in basin analysis I: architecture and genesis of flooding-surface bounded depositional units. *AAPG Bull.* 73, 125–142.

Gómez de Llarena J. 1934: Examples of tertiary tectonic thrust in Asturias, Leon and Palencia. *Bol. R. Soc. Esp. Hist. Nat.* 34, 2–3,123–127 (in Spanish).

Gómez-Fernández F., Méndez-Cecilia A.J. & Bahamonde R.J. 2003: The Boñar Formation (Upper Cretaceous, northern León): Stratigraphy, geochemistry and production potential of natural stone. *Rev. Soc. Geol. Esp.* 16, 1–2, 61–72 (in Spanish with English abstract).

Gossel W., Chudy T. & Falkenhagen M. 2012: Interpolation based on isolines: line-geometry-based inverse distance weighted interpolation (L-IDW) with sample applications from the geosciences. *Z. Dtsch. Ges. Geowiss.* 163, 4, 493–505.

Grijalba-Cuenca A., Torres-Verdín C. & Debeye H.W.J. 2000: Geostatistical inversion of 3-D seismic data to extrapolate petrophysical variables laterally away from the well. *Society of Petroleum Engineers Annual International Meeting Dallas* Texas (October 1–4) SPE Paper 63283, 1–17.

Herrero-Hernández A. 2002: Stratigraphy and sedimentology of the Tertiary deposits of the northern sector of the Duero Basin in the province of León. *PhD. thesis: Universidad de Salamanca*, 1–435 (in Spanish with English abstract).

Herrero-Hernández A. & Gómez-Fernández F. 2012: Palaeoshoreline for the Late Cretaceous marine platform in the Iberian Trough (Leonese Area Spain) deduced from outcrop and subsurface analysis. *Cent. Eur. J. Geosci.* 4, 3, 395–415.

Herrero-Hernández A., Alonso-Gavilán G. & Colmenero R.J. 2004: Subsurface stratigraphy in the northwest sector of the Duero Basin (province of Leon). *Rev. Soc. Geol. Esp.* 17, 3–4, 197–215 (in Spanish with English abstract).

Herrero-Hernández A., Alonso-Gavilán G. & Colmenero R.J. 2010: Depositional sequences in a foreland basin (north-western domain of the continental Duero basin Spain). *Sediment. Geol.* 223, 235–264.

Herrero-Hernández A., Gómez-Fernández F. & López-Moro F.J. 2013: Upper Cretaceous marine-continental transition (Leonese Area NW Spain) defined from integrated outcrop and seismic stratigraphy. *Geol. J.* 50, 39–55

Isaaks E.H. & Srivatava R.M. 1989: An introduction to applied geostatistics *Oxford University Press*, 1–561.

Jonker R.K. 1972: Fluvial sediments of Cretaceous age along the southern border of the Cantabrian Mountains Spain. *Leidse Geologische Mededelingen* 48, 275–379.

Jordan G., Meijninger B.M.L., van Hinsbergen D.J.J., Meulenkamp J.E. & van Dijk P.M. 2005: Extraction of morphotectonic features from DEMs: Development and applications for study areas in Hungary and NW Greece. *Int. J. Appl. Earth Obs.* 7, 163–182.

Jurecka M., Niedzielski T. & Migoń P. 2016: A novel GIS-based tool for estimating present-day ocean reference depth using automatically processed gridded bathymetry data. *Geomorphology* 260, 91–98.

Keller E.A. & Pinter N. 2002: Active Tectonics: earthquakes uplift and landscape. 2nd ed. *Prentice Hall*, 1–359.

Koike K. Nagano S. & Kawaba K. 1998: Construction and analysis of interpreted fracture planes through combination of satellite image derived lineaments and digital elevation model data. *Comput. Geosci.* 24, 573–583.

Krivoruchko K. 2011: Spatial Statistical Data Analysis for GIS Users. *Esri Press*, DVD-ROM.

Lu GY. & Wong DW. 2008: An Adaptive Inverse-Distance Weighting spatial interpolation technique. *Comput. Geosci.* 34, 1044–1055.

Mitchum Jr R.M., Vail P.R. & Thompson III S. 1977: Seismic stratigraphy and global changes of sea-level. Part 2: the depositional sequence as a basic unit for stratigraphic analysis. In: Payton E. (Ed.): Seismic Stratigraphy-Applications to Hydrocarbon Exploration. *AAPG Mem.* 26, 53–62.

Nappi R., Alessio G., Vilardo G. & Bellucci Sessa E. 2009: Integrated morphometric analysis in GIS environment applied to tectonically active areas. *Mem. Soc. Geogr. Ital.* 87, I–II. (in Italian with English abstract).

Sertel E., Demirel H. & Kaya S. 2007: Predictive mapping of air Pollutants: A GIS framework. *Proceedings CD of the Fifth International Spatial Data Quality Symposium* ITC CD Nm.17 Enschede Hollanda 17, 1–5.

Suárez-González, A., Kovács T., Herrero-Hernández A. & Gómez-Fernández F. 2016: Petrophysical characterization of the Dolomitic Member of the Boñar Formation (Upper Cretaceous; Duero Basin, Spain) as a potential CO_2 reservoir. *Estudios Geológicos* 72, 1, e048.

Vail P.R., Mitchum Jr R.M. & Thompson III S. 1977: Seismic stratigraphy and global changes of sea level. Part 3: relative changes of sea level from coastal onlap. In: C.E. Payton (Ed.): Seismic Stratigraphy-Applications to Hydrocarbon Exploration. *AAPG Mem.* 26, 63–81.

Van Ameron H.W.J. 1965: Upper Cretaceous pollen and spores assemblages from the so-called «Wealden» of the pronvience of León (Northern Spain). *Pollen and Spores* 7, 89–93.

Vergés J. & Fernández M. 2006: Ranges and basins in the Iberian Peninsula: their contribution to the present topography. In: Gee D.G. & Stephenson R.A. (Eds.): European Lithosphere Dynamics. *Geol. Soc. London, Mem.* 32, 223–234.

Webster R. & Oliver M.A. 2001: Geostatistics for environmental scientists. *John Wiley and Sons Ltd*., Chichester, 1–271.